Fabrication of Cellulose Nanocrystals (CNCs) in Choline Chloride-Citric Acid (ChCl-CA) Solvent to Lodge Antimicrobial Activity

Yuanchen Zhu,[a,b] Jinhui Zhang,[a,b] Ping Zhao,[a,b] Dawei Wang,[a,b] Zhengjun Shi,[c] Jing Yang,[a,b] and Haiyan Yang [a,b,*]

Surface-modified cellulose nanocrystals (CNCs) have gained substantial interest in industry. The renewability and abundance of the raw material to prepare CNCs make them a promising green material. In this study, two types of CNCs were prepared by sulfuric acid (H_2SO_4) and stepwise H_2SO_4 and choline chloride-citric acid (ChCl-CA) deep eutectic solvent-like (DES) treatments. The DES treatment led to esterification and further degradation of the CNCs. The obtained nanoparticles were distributed in size range of 50 nm to 500 nm and 20 nm to 70 nm for the H_2SO_4 and stepwise treatments, respectively. The effects of the nanoparticles on the mechanical properties, thermal stability, and antibacterial activity of poly(vinyl alcohol) (PVOH) were determined using a universal mechanical testing machine, thermogravimetric analysis (TGA), and the agar diffusion method. The results indicated that nanoparticles had good compatibility in PVOH at a concentration below 10%. The CNCs had greater effect on the mechanical properties and the thermal stability of films than the esterified CNCs. However, the CA modified CNCs showed more favorable antibacterial activity than the CNCs from H_2SO_4 treatment. Taking the mechanical properties, the thermal stability, and the antibacterial activity into consideration, 5% was selected as a suitable concentration for composite film preparation.

DOI: 10.15376/biores.17.3.4347-4359

Keywords: Cellulose nanocrystals; Deep eutectic solvent; Composite film; Antibacterial activity

Contact information: a: Key Laboratory for Forest Resources Conservation and Utilization in the Southwest Mountains of China, Ministry of Education, Southwest Forestry University, Kunming 650224, China; b: College of Chemical Engineering, Southwest Forestry University, Kunming, 650224, China; c: Key Laboratory for Forest Resources Conservation and Utilization in the Southwest Mountains of China, Ministry of Education, Southwest Forestry University, Kunming, 650224, China;
** Corresponding author: yanghaiyan@swfu.edu.cn*

INTRODUCTION

Cellulose is the most abundant organic polymer on earth and a promising renewable resource for the production of biobased materials and fuels (Jacob *et al.* 2004). Cellulose is a linear polymer of hydroglucose units linked by β-1,4-glycoside bonds. The cellulose chains assemble through intra- and intermolecular hydrogen bonds, leading to a coexistence of crystalline and amorphous regions within cellulose fibers (Klemm *et al.* 2005; Habibi 2014). The microscopic properties of cellulose make it widely used in various areas. Traditionally, cellulose has been extensively used as a raw material for lumber and textiles for thousands of years. The growing world population and rapid technological growth has driven research on the use of cellulose as a raw material in products including

paper, cellophane films, explosives, and dietary fibers (Reishofer *et al.* 2017). Recently, nanosized and high crystalline cellulose with high rigidity, tensile stiffness, and shear force has attracted much attention due to its intrinsic properties (Habibi 2014; Wang *et al.* 2018). Thus, cellulose nanocrystals (CNCs) can be used as a reinforcing material to improve surface and antifouling properties of polymers (Jin *et al.* 2016; Rodrigues *et al.* 2017; Bai *et al.* 2019). In addition, CNCs possess hydroxyl groups and can be modified by oxidation, esterification, etherification, and grafting copolymerization (Liu *et al.* 2017a). Previous research has reported that cellulose possesses good antibacterial properties and durability after modification with metals (Emam *et al.* 2014, 2015).

In addition, cellulose can be disintegrated into substructural fibrils by mechanical treatments, chemo-mechanical treatments, and enzymatic-mechanical treatments (Thomas *et al.* 2018). Among these technologies, mechanical treatment is limited in nanocellulose production due to its high energy consumption and cost (Spence *et al.* 2011). Acid hydrolysis is the most common chemical treatment employed to obtain CNCs, and concentrated sulfuric acid (H_2SO_4) (64%) is the common reagent in the industrial production of CNCs (Rånby 1951). During acid treatment, the surface hydroxyl groups of CNCs are partially functionalized, conferring surface charges and aqueous suspendability of CNCs. However, the corrosive nature of acid and large amounts of chemical waste products are current limitations of the acid hydrolysis process (Thomas *et al.* 2018).

Recently, deep eutectic-like solvents (DESs) have become recognized as promising media for nanoparticle fabrication (Abo-Hamad *et al.* 2015; Hammond *et al.* 2017). The term eutectic-like needs to be used here because typically the ratio of components in DES formulations does not correspond to the eutectic point. DESs consist of a hydrogen bond donor (HBD) and a hydrogen bond acceptor (HBA) pair and can be tailored by adjusting the properties of the HBD and HBA. They are often considered to be analogous to ionic liquids (ILs), which exhibit a low vapor pressure and a good solvent capability for chemical synthesis (Hong *et al.* 2020). Among the DES systems, quaternary ammonium salt and a hydrogen bond donor make up type III DESs. These compositions are biodegradable and have a low toxicity. Topically, DESs formed from carboxylic acids can be used as a hydrolytic medium to produce CNCs (Sirviö *et al.* 2016). In addition, the carboxylic acid-based DESs can also be used to prepare cellulose nanofibers (CNFs) accompanied by simultaneous esterification modifications of CNFs (Liu *et al.* 2021).

In this study, microcrystalline cellulose (MCC) was pretreated with H_2SO_4 and stepwise H_2SO_4 and choline chloride-citric acid (ChCl-CA) DES, respectively. The characteristics of the obtained CNCs samples were analyzed by Fourier transform infrared spectrometry (FTIR) and transmission electron microscopy (TEM). The effect of the two CNCs samples on the surface features, thermal stabilities, transparencies, and mechanical properties of poly(vinyl alcohol) (PVOH)-CNC composite films were investigated by scanning electron microscopy (SEM), a simultaneous thermal analyzer, and a universal mechanical testing machine. The antibacterial activities of the composite films were also analyzed by the agar diffusion method.

EXPERIMENTAL

Modification of Microcrystalline Cellulose

Before modification, the MCC (Supelco, Bellefonte, PA, USA) was pretreated with H_2SO_4. In detail, 10 g of MCC and 150 mL of H_2SO_4 solution (64% w/w) were put into a

flask and incubated in water bath at 44 °C under stirring for 1 h. After incubation, the solution was dispersed in 1,500 mL of distilled water to form a suspension. Then, the suspension was collected by centrifugation, followed by dialysis to remove the excess acid. The samples then were freeze-dried. The obtained samples were labeled as CNCs.

The modification of the CNCs was conducted by mixing 1 g of CNCs and 40 mL of ChCl-CA DES (prepared by mixing ChCl and CA at ratio of 1:1, Shanghai Macklin Biochemical Co., Ltd., Shanghai, China) at 120 °C for 8 h under stirring. After the reaction, the precipitate was centrifuged for several times and washed with ethanol and water to remove the DES until the suspension was neutralized. Then, freeze-dried the precipitate and labeled as CA-CNCs.

Preparation of the PVOH Composite Films

To prepare the PVOH composite films, 1 g of PVOH powder (Shanghai Chenqi Chemical Technology Co., Ltd., Shanghai, China) was added into 10 mL of water and stirred continuously at 90 °C for 1 h to obtain a 10% PVOH solution. Then, 15 mL suspension solutions containing 0.01, 0.05, and 0.1 g of CNCs and CA-CNCs were added into the PVOH solution. The mixture solutions were stirred for 1 h and further ultrasonic treated for 5 min to eliminate bubbles for the film preparation. The films were obtained by pouring the solutions into the petri dish, drying them at 40 °C for 24 h and stripping them from the dish. The obtained films were labeled as PVOH, PVOH-1CNCs, PVOH-5CNCs, PVOH-10CNCs, PVOH-1CA-CNCs, PVOH-5CA-CNCs, and PVOH-10CA-CNCs according to the concentration and type of CNCs. The composite films were stored in a drying oven for further analysis.

Analysis Procedures

The FTIR spectra of the CA, CNCs, and CA-CNCs were recorded with a Nicolet Is50 infrared spectrometer (Thermo Fisher Scientific, Waltham, MA, USA) at a resolution of 4 cm^{-1} in the frequency range of 4000 to 500 cm^{-1}. The samples were mixed with potassium bromide and ground to a fine powder to approximately 1% concentration.

Bright field images of the CNCs and CA-CNCs were taken with a Zeiss Libra 200EF transmission electron microscope (TEM) (Jena, Germany). The TEM grids were prepared by dispersing the CNCs and CA-CNCs at 1% concentration in water and then placing them in a Novascan PSDP-UV8T UV-ozone system (Ames, IA, USA) at room temperature for 30 min using a 400-mesh copper grid carbon (3 nm to 4 nm) and a Formvar (Ames, IA, USA) film coating (25 nm to 50 nm).

The SEM images of the composite films were obtained with a Zeiss Libra Sigma 300 microscope (Jena, Germany) at an accelerated voltage of 15 kV. Each sample was coated with a thin platinum conductive layer before it was examined. Due to the heterogeneity of the samples, several pictures were taken of each sample and only representative photos were presented.

The mechanical properties of the films were tested with a universal mechanical testing machine (ETM Type D; Wance, Shenzhen, China). The tensile strength, elongation at break, and other mechanical properties of the film were analyzed. Prior to analysis, the films were dried at 40 °C, cut into rectangular slices (100 mm × 15 mm) with an average thickness of 0.12 mm, and analyzed at a rate of 10 mm/min.

The thermal stabilities of the composite films were analyzed on a simultaneous thermal analyzer (TG209F3; NETZSCH, Selb, Germany). The samples weighed between

8 and 10 mg and were run from 30 to 600 °C at a heating rate of 10 °C/min in a nitrogen atmosphere.

Antibacterial Activity

The antibacterial activities of the pure PVOH and nanocomposite PVOH films were tested against gram-negative bacteria (*Escherichia coli*) by the agar diffusion method (Bauer *et al.* 1966). Before inoculating, the bacterial was incubated in nutrient agar medium at 37 °C for 24 h and diluted to 100 CFU/mL. 0.1 mL bacterial suspension was added into the nutrient agar medium before films (which were cut into 6 mm circular disc) were placed on each medium. This system was further incubated at 37 °C for 24 h. The diameter of the inhibition zones was measured to investigate the antimicrobial activities of films with different proportions of CNCs samples. The measurement consisted of three replicates and the standard deviations were also determined.

RESULTS AND DISCUSSION

FTIR Analysis of the CNCs and CA-CNCs

The possible changes in the structure of the MCC after H_2SO_4 and stepwise H_2SO_4-DES treatments were determined by FTIR analysis. The FTIR spectra of the CA, CNCs, and CA-CNCs samples are comparatively shown in Fig. 1. The strong broad peak at approximately 3300 cm^{-1} is assigned to the free -OH stretching and bending vibration of the hydroxyl groups in all the samples (Tenhunen *et al.* 2018). The peak at 2900 cm^{-1} is related to the stretching of alkyl groups. The intensity of the 1429 cm^{-1} is related to the bending and scissoring of the $–CH_2–$ groups. The characteristic peaks of cellulose are observed at peaks 1371, 1163, 1112, 1056, and 898 cm^{-1}. These peaks are due to the C–H bending vibration (1371 cm^{-1}), the C–O tensile vibration (1163, 1112 and 1056 cm^{-1}), the ring-shaped tensile vibration (898 cm^{-1}), respectively (Yu *et al.* 2019). Compared with the FT-IR spectrum of CNCs, the absorbance of the peak at 1730 cm^{-1} in the spectrum of CA-CNCs is associated with the carbonyl vibrations of ester (Sirviö *et al.* 2016). This phenomenon indicates esterification of hydroxyl groups of cellulose with CA during the DES pretreatment. The esterification of hydroxyl groups of cellulose has also been observed in the research of carboxylic acid-based DESs pretreated with cellulose for the production of cellulose nanofibrils (Liu *et al.* 2021; Yu *et al.* 2021a). This result suggested that the CA had a dual function as a hydrogen bonded donor and reactant for cellulose esterification.

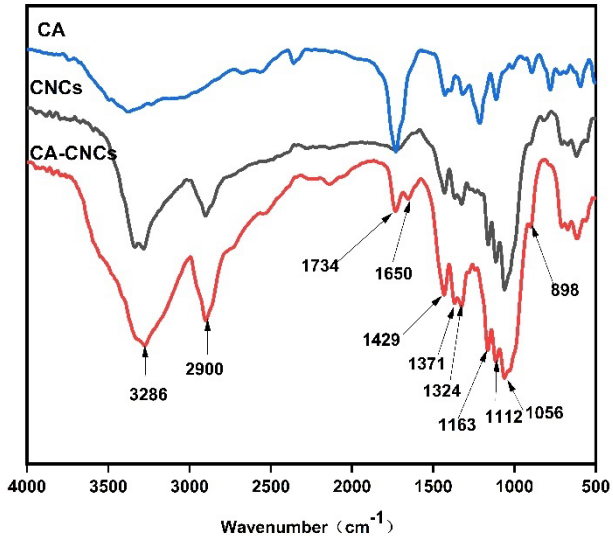

Fig. 1. The FTIR spectra of the CA, CNCs, and CA-CNCs samples obtained by the H_2SO_4 pretreatment and the stepwise H_2SO_4 and DES treatments

TEM Analysis of the CNCs and CA-CNCs

The microscopic morphology of residues obtained by the H_2SO_4 and H_2SO_4-DES stepwise pretreatments were analyzed by TEM. The products are observed as aggregates. This was attributed to the abundance of surface hydroxyl groups (Wohlhauser *et al.* 2018). The H_2SO_4 treatment of the MCC yielded particle with size of 50 nm to 500 nm, of which 45% is observed in size of 200 nm to 300 nm (Figs. 2a and 2c). This result suggests that the residues obtained from sulfuric acid were CNCs (He *et al.* 2018). The sample obtained by the stepwise H_2SO_4 and DES treatments had smaller particles (20 nm to 70 nm) as compared to the sample obtained from the H_2SO_4 treatment (Figs. 2b and 2d). This result indicates that the CNCs backbone was further degraded by the acidic ChCl-CA DES. The degradation of cellulose during acidic DES pretreatment was also reported in other researches (Ling *et al.* 2020; Oh *et al.* 2020). Furthermore, a hydrogen bond donor with more carboxyl groups leads to stronger acidity of DES solution, yielding more degradation of cellulose as compared to monomeric acid (Oh *et al.* 2020). These CNCs are expected to play as efficient reinforcement agents at low filler loading levels in polymeric systems (Neto *et al.* 2013).

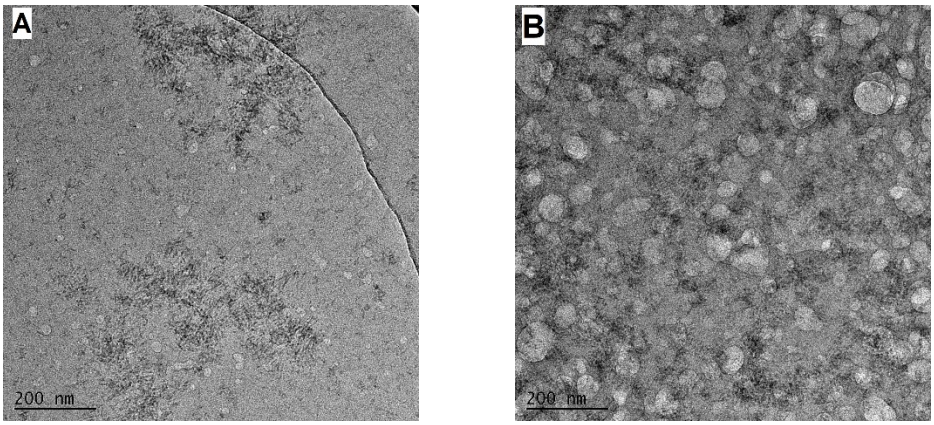

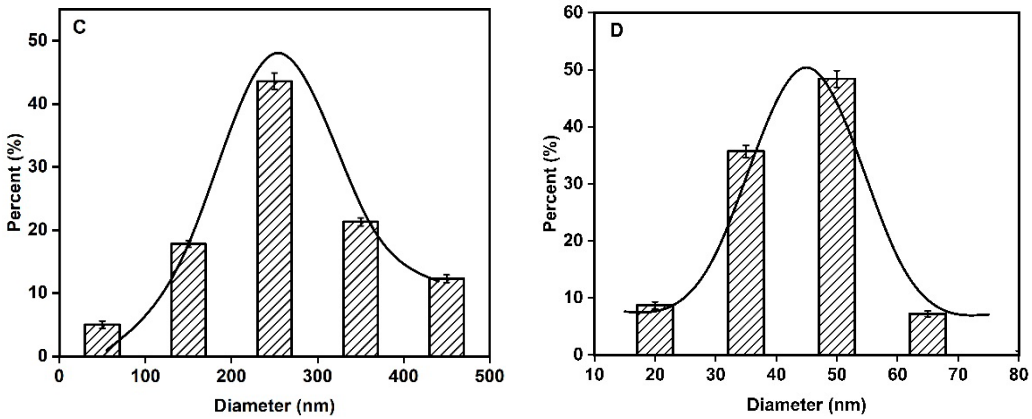

Fig. 2. TEM images and size distribution of the CNCs (A,C) and CA-CNCs (B,D) samples obtained by the H_2SO_4 pretreatment and stepwise H_2SO_4 and DES treatments

Surface Features and Mechanical Properties of the Films

The morphologies of the PVOH composite films with different contents of CNCs and CA-CNCs were investigated through SEM. Figure 3 shows the magnified imaging for better visual understanding of the samples. The PVOH and PVOH composites with a low concentration of nanoparticles films (1% and 5%) had a smoother surface. Some particles are observed on the surface of films with 10% CNCs and CA-CNCs. These results suggested that nanoparticles at a concentration of 1% and 5% had good diffusion in PVOH. However, when the concentration of nanoparticles was increased to 10%, some of them were present on the surface of the PVOH. This result is consistent with previous reports that the CNCs may self-aggregate and show poor compatibility at loadings higher than 3 wt.%. This has been attributed to the large amount of hydroxyl groups on the cellulose surface (Dufresne 2013; Song *et al.* 2014). However, such an explanation does not account for the dependency of agglomeration on the CNC concentration.

The mechanical properties of the films, including the stress, tensile strength, strain, and Young's modulus are displayed in Fig. 4. The tensile strength of the films increased from 64 MPa to 75 MPa and 91 MPa with CNCs dosages of 1% and 5%, respectively. At the same dosages, the CA-CNCs increased the tensile strength of the films to 69 and 77 MPa, respectively. This result might be ascribed to the fact that larger size of CNCs shown in Fig. 2 corresponds to larger aspect ratio of it, showing a favorable enhancement of mechanical properties of films than CA-CNCs. However, the tensile strength of the films decreased to 30 and 25 MPa as the nanoparticle concentration reached 10%, respectively. A similar relationship between the nanocellulose content and the mechanical properties of films was reported by Sarwar *et al.* (2018). The increased tensile strength of the composite films is ascribed to the fact that CNCs and CA-CNCs nanoparticles create interfacial hydrogen bonds with the PVOH matrix, anchoring the PVOH chain against movement. The results are attributed the fact that a large amount of intermolecular bonding between the fibers and the PVOH matrix originate from good dispersion of nanoparticles (Asrofi *et al.* 2018; Abral *et al.* 2019). The dispersion condition of fiber was confirmed by the SEM analysis. Moreover, the improvement of the tensile strength with increased nanocomposite content was due to the inherent chain stiffness and rigidity in the CNCs and CA-CNCs, and the homogenous distribution of nanofiller in the polymer matrix (Mandal and Chakrabarty 2014). An enhancement of storage modulus of starch films was also achieved by compositing starch and sucrose (Wu *et al.* 2018; Zhou *et al.* 2009).

The reduction in the tensile strength may be ascribed to the agglomeration of cellulose at a high proportion in the PVOH matrix. In addition, an excessive amount of nanocellulose might break the interaction of the PVOH matrix, reducing the tensile strength of the films (Frone *et al.* 2011). The strain break decreased with the increase of CNCs and CA-CNCs concentration in the films. This phenomenon has also been observed in the mechanical properties of PVOH/CNC composite films (Kim *et al.* 2019).

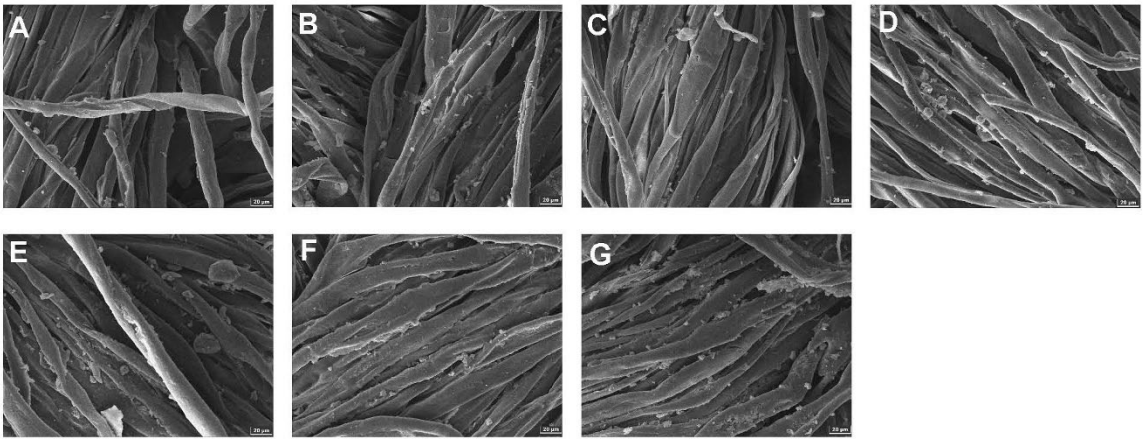

Fig. 3. The SEM images of the A) PVOH, B) PVOH-1CNCs, C) PVOH-1CA-CNCs, D) PVOH-5CNCs, E) PVOH-5CA-CNCs, F) PVOH-10CNCs, and G) PVOH-10CA-CNCs composite films

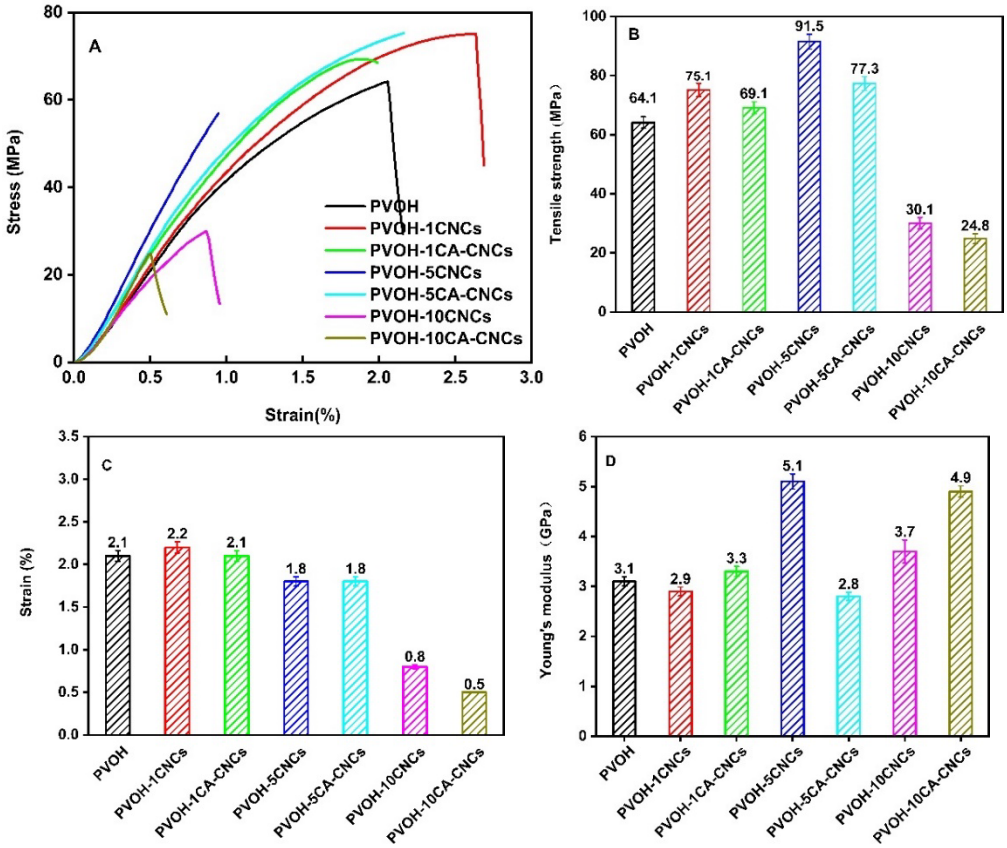

Fig. 4. The A) stress, B) tensile strength, C) strain, and D) Young's modulus mechanical properties of the composite films with different contents of CNCs and CA-CNCs

Thermal Stabilities of Films

The thermogravimetric (TG) and derivative thermogravimetric (DTG) curves of the PVOH composite films with different CNC and CA-CNC contents are illustrated in Fig. 5. The decomposition of the films contained three phases, which correspond to the elimination and dehydration, radical, and cyclization reactions (Gilman *et al.* 1995). The weight loss peak that occurred at approximately 100 °C corresponds to the evaporation of absorbed water. The major weight loss focused between 250 and 450 °C was attributed to the thermal decomposition of PVOH, which is the main component of the films. Pyrolysis of films started at approximately 250 °C and the degradation rate increased with temperature, obtaining a maximum degradation rate at approximately 320 °C. In addition, the degradation of cellulose was also observed in this region (Cuilty *et al.* 2018). A slight shift of temperature peak at the maximum degradation rate was observed as composing nanoparticles in the films. This could be attributed to the fact that the nanoparticles slightly improved the thermal resistances of the films (Abral *et al.* 2019). The degradation temperature increased as the concentration of nanoparticles increased to 5% in the film. However, the films with 10% nanoparticles showed a similar stability as the pure PVOH film. This result was consistent with the results of the SEM analysis. Nanoparticles diffused in the PVOH improved the thermal stability of the composite films. The participated nanoparticles on the surface of the PVOH showed a negligible effect on the thermal stability of the composite films. These results also indicated that 5% was the favorable nanoparticles concentration in the PVOH film. Meanwhile, films composed of the CNCs had a slightly higher stability than the films composed of the CA-CNCs. This result might be ascribed to the larger size of the CNCs as compared to the CA-CNCs, which is consistent with the results shown in the TEM images (Fig. 2). The third weight loss peak at approximately 430 °C corresponds to the decomposing of the cellulose. At this temperature, cellulose can decompose into D-glucopyranose monomers and then into free radicals (Das *et al.* 2014). This may also be ascribed to the decomposition of ash (Syafri *et al.* 2019).

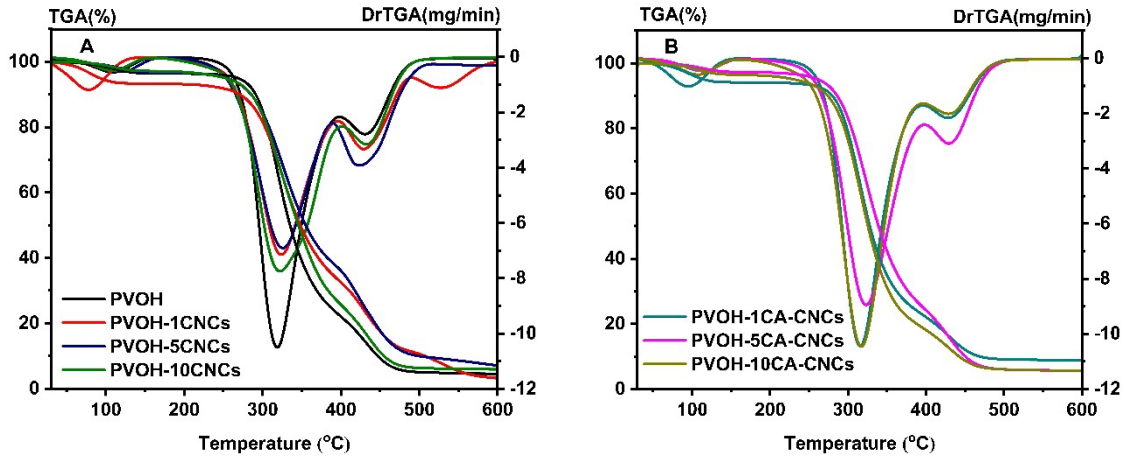

Fig. 5. The TG and DTG curves of the A) PVOH, PVOH-1CNCs, PVOH-5CNCs, and PVOH-10CNCs and B) PVOH-1CA-CNCs, PVOH-5 composite films

Antibacterial Activities of the Films

Antibacterial activity is one of the most important properties for film as it used in food packaging. The antibacterial activities of the films with different proportions of CNCs

and CA-CNCs against Gram negative bacteria (*E. coli*) are shown in Fig. 6. The inhibitory effect was measured based on the clear zone surrounding the circular film disc. The inhibition zones of the films with CNCs and a low concentration of CA-CNCs (1%) were not clear. The activity increased as the concentration of the CA-CNCs nanoparticles increased. As the CA-CNCs dosage increased to 5% and 10%, the inhibition zone was clearly observed (Fig. 6g). The antibacterial activity of films was ascribed to the CA graft of the CA-CNCs. Crosslinking CA and electrospun PVOH microfiber mats also exhibited strong antibacterial activity (Yu *et al.* 2021b).

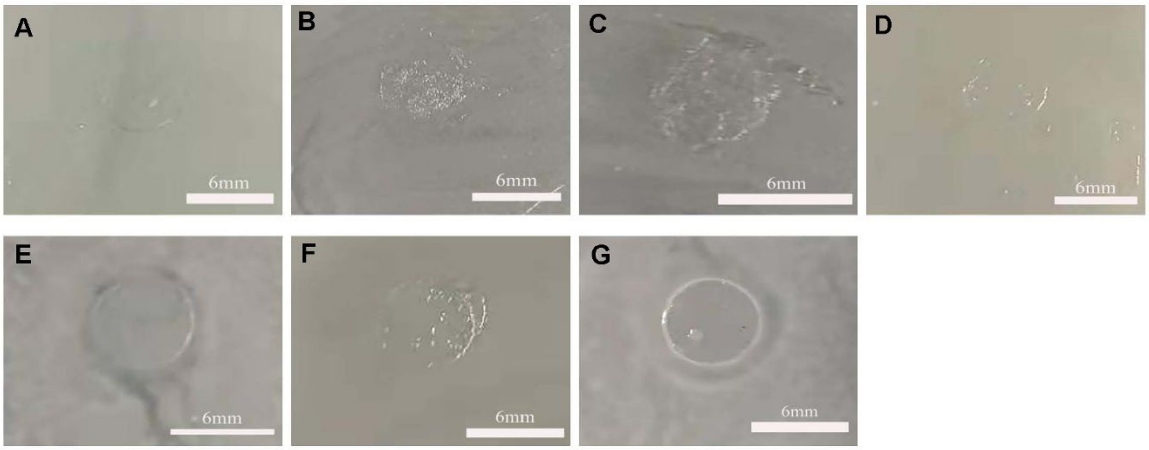

Fig. 6. The antibacterial activities of the A) PVOH, B) PVOH-1CNCs, C) PVOH-1CA-CNCs, D) PVOH-5CNCs, E) PVOH-5CA-CNCs, F) PVOH-10CNCs, and G) PVOH-10CA-CNCs composite films

CONCLUSIONS

1. Deep eutectic-like solvent (DES) treatment introduced esterification and further degradation of cellulose nanocrystals (CNCs), resulting in a decreased size of the esterified CNCs in size range of 20 to 70 nm.
2. Compositing the modified CNCs nanoparticles with poly(lactic acid) (PLA) introduced enhanced mechanical properties of PLA films. As the nanoparticle content increased to 5%, the tensile strength and Young's modulus of composite films increased from 64 MPa to 91 MPa and 3 MPa to 5 GPa, respectively.
3. The mechanical properties of the films decreased as the concentration of particles reached 10%. However, composite films with this concentration of esterified CNCs showed antibacterial activity properties.
4. Esterified citric acid (CA)-CNCs had favorable antibacterial activity as compared to the default CNCs.
5. Taking the mechanical properties and the thermal stabilities of the film into consideration, 5% was judged to be the favorable concentration of nanoparticles in the PVOH film.

ACKNOWLEDGMENTS

The authors are grateful for the support of the Applied Basic Research Key Project of Yunnan Province (Grant Nos. 202201AT070052, 202101BD070001-076), the Yunnan Province Department of Education (2020J0398), the Key Laboratory of State Forestry and Grassland Administration on Highly-Efficient Utilization of Forestry Biomass Resource in Southwest China (2020-KF05), the Key Laboratory for Forest Resources Conservation and Utilization in the Southwest Mountains of China, the Ministry of Education, Southwest Forestry University (KLESWFU-201807), and the National Natural Science Foundation of China (Grant Nos. 31971741 and 31760195).

REFERENCES CITED

Abo-Hamad, A., Hayyan, M., AlSaadi, M. A., and Hashim, M. A. (2015). "Potential applications of deep eutectic solvents in nanotechnology," *Chemical Engineering Journal* 273, 551-567. DOI: 10.1016/J.cej.2015.03.091

Abral, H., Kadriadi, Mahardika, M., Handayani, D., Sugiarti, E., and Muslimin, A. N. (2019). "Characterization of disintegrated bacterial cellulose nanofibers/PVOH bionanocomposites prepared via ultrasonication," *International Journal of Biological Macromolecules* 135, 591-599. DOI: 10.1016/j.ijbiomac.2019.05.178

Asrofi, M., Abral, H., Kasim, A., Pratoto, A., Mahardika, M., and Hafizulhaq, F. (2018). "Mechanical properties of a water hyacinth nanofiber cellulose reinforced thermoplastic starch bionanocomposite: Effect of ultrasonic vibration during processing," *Fibers* 6(2), 40-48. DOI: 10.3390/fib6020040

Bai, L., Liu, Y., Ding, A., Ren, N., Li, G., and Liang, H. (2019). "Surface coating of UF membranes to improve antifouling properties: A comparison study between cellulose nanocrystals (CNCs) and cellulose nanofibrils (CNFs)," *Chemosphere* 217, 76-84. DOI: 10.1016/j.chemosphere.2018.10.219

Bauer, A. W., Kirby, W. M. M., Sherris, J. C., and Turck, M. (1996). "Antibiotic susceptibility testing by a standardized single disk method," *American Journal of Clinical Pathology* 45(4), 493-496. DOI: 10.1093/ajcp/45.4_ts.493

Cuilty, K. R., Ballinas-Casarrubias, L., Miguel, E. R. S., de Gyves, J., Robles-Venzor, J. C., and González-Sánchez G. (2018). "Cellulose recovery from *Quercus* sp. sawdust using ethanosolv pretreatment," *Biomass and Bioenergy* 111, 114-124. DOI: 10.1016/j.biombioe.2018.02.004

Das, A. M., Ali, A. A., and Hazarika, M. P. (2014). "Synthesis and characterization of cellulose acetate from rice husk: Eco-friendly condition," *Carbohydrate Polymers* 112, 342-349. DOI: 10.1016/j.carbpol. 2014.06.006

Dufresne, A. (2013). "Nanocellulose: A new ageless bionanomaterial," *Materials Today* 16(6), 220-227. DOI: 10.1016/j.mattod.2013.06.004

Emam, H. E., Manian, A. P., Široká, B., Duelli, H., Merschak, P., Redl, B., and Bechtold, T. (2014). "Copper(I)oxide surface modified cellulose fibers– Synthesis, characterization and antimicrobial properties," *Surface and Coatings Technology* 254, 344-351. DOI: 10.1016/j.surfcoat.2014.06.036

Emam, H. E., El-Rafie, M. H, Ahmed, H. B., and Zahran, M. K. (2015). "Room temperature synthesis of metallic nanosilver using acacia to impart durable biocidal

effect on cotton fabrics," *Fibers and Polymers* 16(8), 1676-1687. DOI: 10.1007/s12221-015-5197-x

Frone, A. N., Panaitescu, D. M., Donescu, D., Spataru, C. I., Radovici, C., Trusca, R., and Somoghi, R. (2011). "Preparation and characterization of PVOH composites with cellulose nanofibers obtained by ultrasonication," *BioResources* 6(1), 487-512. DOI: 10.15376/biores.6.1.487-512

Gilman, J. W., VanderHart, D. L., and Kashiwagi, T. (1995). "Thermal decomposition chemistry of poly (vinyl alcohol)," in: *Fire and Polymers II*, G. L. Nelson (ed.), American Chemical Society, Washington, DC, USA, pp. 161-185. DOI: 10.1021/bk-1995-0599.ch011

Habibi, Y. (2014). "Key advances in the chemical modification of nanocelluloses," *Chemical Society Reviews* 43(5), 1519-1542. DOI: 10.1039/C3CS60204D

Hammond, O. S., Edler, K. J., Bowron, D. T., and Torrente-Murciano, L. (2017). "Deep eutectic-solvothermal synthesis of nanostructured ceria," *Nature Communications* 8, 14150. DOI: 10.1038/ncomms14150

He, X., Luzi, F., Yang, W., Xiao, Z., Torre, L., Xie, Y., and Puglia, D. (2018). "Citric acid as green modifier for tuned hydrophilicity of surface modified cellulose and lignin nanoparticles," *ACS Sustainable Chemistry & Engineering* 6(8), 9966-9978. DOI: 10.1021/acssuschemeng.8b01202

Hong, S., Yuan, Y., Li, P., Zhang, K., Lian, H., and Liimatainen, H. (2020). "Enhancement of the nanofibrillation of birch cellulose pretreated with natural deep eutectic solvent," *Industrial Crops and Products* 154, 112677. DOI: 10.1016/j.indcrop.2020.112677

Jacob, M., Thomas, S., and Varughese, K.T. (2004). "Mechanical properties of sisal/oil palm hybrid fiber reinforced natural rubber composites," *Composite Science and Technology* 64(7-8), 955-965. DOI: 10.1016/S0266-3538(03)00261-6

Jin, Z., Fan, H., Li, B.-G., and Zhu, S. (2016). "Evaluation of octylteramethyldisiloxane-containing ethylene copolymers as composite lubricant for high-density polyethylene," *Macromolecular Materials and Engineering* 301(12), 1494-1502. DOI: 10.1002/mame.201600292

Kim, J. W., Park, H., Lee, G., Jeong, Y. R., Hong, S. Y., Keum, K., Yoon, J., Kim, M. S., and Ha, J. S. (2019). "Paper-like, thin, foldable, and self-healable electronics based on PVOH/CNC nanocomposite film," *Advanced Functional Materials* 29(50), 1905968. DOI: 10.1002/adfm.201905968

Klemm, D., Heublein, B., Fink, H.-P., and Bohn, A. (2005). "Cellulose: Fascinating biopolymer and sustainable raw material," *Angewandte Chemie* 44(22), 3358-3393. DOI: 10.1002/anie.200460587

Ling, Z., Guo, Z., Huang, C., Yao, L., and Feng, X. (2020). "Deconstruction of oriented crystalline cellulose by novel levulinic acid based deep eutectic solvents pretreatment for improved enzymatic accessibility," *Bioresource Technology* 305, 123025. DOI: 10.1016/j.biortech.2020.123025

Liu, S., Zhang, Q., Gou, S., Zhang, L., and Wang, Z. (2021). "Esterification of cellulose using carboxylic acid-based deep eutectic solvents to produce high-yield cellulose nanofibers," *Carbohydrate Polymers* 251, 117018. DOI: 10/1016/j.carpol.2020.117018

Liu, Y., Huang, H., Huo, P., and Gu, J. (2017a). "Exploration of zwitterionic cellulose acetate antifouling ultrafiltration membrane for bovine serum albumin (BSA)

separation," *Carbohydrate Polymers* 165, 266-275. DOI: 10.1016/j.carbpol.2017.02.052

Liu, Y., Guo, B., Xia, Q., Meng, J., Chen, W., Liu, S., Wang, Q., Liu, Y., Li, J., and Yu, H. (2017b). "Efficient cleavage of strong hydrogen bonds in cotton by deep eutectic solvents and facile fabrication of cellulose nanocrystals in high yields," *ACS Sustainable Chemistry & Engineering* 5(9), 7623-7631. DOI: 10.1021/acssuschemeng.7b00954

Mandal, A., and Chakrabarty, D. (2014). "Studies on the mechanical, thermal, morphological and barrier properties of nanocomposites based on poly(vinyl alcohol) and nanocellulose from sugarcane bagasse," *Journal of Industrial Engineering Chemistry* 20(2), 462-473. DOI: 10.1016/j.jiec.2013.05.003

Neto, W. P. F., Silvério, H. A., Dantas, N. O., and Pasquini, D. (2013). "Extraction and characterization of cellulose nanocrystals from agro-industrial residue – Soy hulls," *Industrial Crops and Products* 42, 480-488. DOI: 10.1016/j.indcrop.2012.06.041

Oh, Y., Park, S., Jung, D., Oh, K. K., and Lee, S. H. (2020). "Effect of hydrogen bond donor on the choline chloride-based deep eutectic solvent-mediated extraction of lignin from pine wood," *International Journal of Biological Macromolecules* 165(A), 187-197. DOI: 10.1016/j.ijbiomac.2020.09.145

Rånby, B. G. (1951). "Fibrous macromolecular systems. Cellulose and muscle. The colloidal properties of cellulose micelles," *Discussions of the Faraday Society* 11, 158-164. DOI: 10.1039/df9511100158

Reishofer, D., Ehmann, H. M., Amenitsch, H., Gspan, C., Fischer, R., Plank, H., Trimmel, G., and Spirk, S. (2017). "On the formation of Bi_2S_3-cellulose nanocomposite film from bismuth xanthates and trimethylsilyl-cellulose," *Carbohydrate Polymers* 164, 294-300. DOI: 10.1016/j.carbpol.2017.02.008

Rodrigues, A. P. H, de Souza, S. D., Gil, C. S. B., Pereira, F. V., de Oliveira L. C. A., and Patricio, P. S. D. (2017). "Biobased nanocomposites based on collagen, cellulose nanocrystals, and plasticizers," *Journal of Applied Polymer Science* 134(25), 1-9. DOI: 10.1002/app.44954

Sarwar, M. S., Niazi, M. B. K., Jahan, Z., Ahmad, T., and Hussain, A. (2018). "Preparation and characterization of PVOH/nanocellulose/Ag nanocomposite films for antimicrobial food packaging," *Carbohydrate Polymers* 184, 453-464. DOI: 10.1016/j.carbpol.2017.12.068

Sirviö, J. A., Visanko, M., and Liimatainen, H. (2016). "Acidic deep eutectic solvents as hydrolytic media for cellulose nanocrystal production," *Biomacromolecules* 17(9), 3025-3032. DOI: 10.1021/acs.biomac.6b00910

Song, Z., Xiao, H., and Zhao, Y. (2014). "Hydrophobic-modified nano-cellulose fiber/PLA biodegradable composites for lowering water vapor transmission rate (WVTR) of paper," *Carbohydrate Polymers* 111, 442-448. DOI: 10.1016/j.carbpol.2014.04.049

Spence, K. L., Venditti, R. A., Rojas, O. J., Habibi, Y., and Pawlak, J. J. (2011). "A comparative study of energy consumption and physical properties of microfibrillated cellulose produced by different processing methods," *Cellulose* 18(4), 1097-1111. DOI: 10.1007/s10570-011-9533-z

Syafri, E., Kasim, A., Abral, H., and Asben, A. (2019). "Cellulose nanofibers isolation and characterization from ramie using a chemical ultrasonic treatment," *Journal of Natural Fibers* 16(8), 1145-1155. DOI: 10.1080/15440478.2018.1455073

Tenhunen, T.-M., Lewandowska, A. E., Orelma, H., Johansson, L.-S., Virtanen, T., Harlin, A., Österberg, M., Eichhorn, S. J., and Tammelin, T. (2018). "Understanding the interactions of cellulose fibers and deep eutectic solvent of choline chloride and urea," *Cellulose* 25(1), 137-150. DOI: 10.1007/s10570-017-1587-0

Thomas, B., Raj, M. C., Athira, K. B., Rubiyah, M. H., Joy, J., Moores, A., Drisko, G. L., and Sanchez, C. (2018). "Nanocellulose, a versatile green platform: From biosources to materials and their applications," *Chemical Reviews* 118(24), 11575-11625. DOI: 10.1021/acs.chemrev.7b00627

Wang, Y., Wang, X., Xie, Y., and Zhang, K. (2018). "Functional nanomaterials through esterification of cellulose: A review of chemistry and application," *Cellulose* 25(7), 3703-3731. DOI: 10.1007/s10570-018-1830-3

Wohlhauser, S., Delepierre, G., Labet, M., Morandi, G., Thielemans, W., Weder, C., and Zoppe, J. O. (2018). "Grafting polymers from cellulose nanocrystals: Synthesis, properties, and applications," *Macromolecules* 51(16), 6157-6189. DOI: 10.1021/acs.macromol.8b00733

Wu, M., Gao, F., Yin, D. M., Luo, Q., Fu, Z. Q., and Zhou, Y. G. (2018). "Processing of superfine grinding corn straw fiber-reinforced starch film and the enhancement on its mechanical properties," *Polymer* 10(8), 855. DOI: 10.3390/polym10080855

Yu, W., Wang, C., Yi, Y., Zhou, W., Wang, H., Yang, Y., and Tan, Z. (2019). "Choline chloride-based deep eutectic solvent systems as a pretreatment for nanofibrillation of ramie fibers," *Cellulose* 26(5), 3069-3082. DOI: 10.1007/s10570-019-02290-7

Yu, D., Feng, Y.-Y., Xu, J.-X., Kong, B. H., Liu, Q., and Wang, H. (2021a). "Fabrication, characterization, and antibacterial properties of citric acid crosslinked PVOH electrospun microfibre mats for active food packaging," *Packaging Technology and Science* 34(6), 361-370. DOI: 10.1002/pts.2566

Yu, W., Wang, C., Yi, Y., Wang, H., Yang, Y., Zeng, L., and Tan, Z. (2021b). "Direct pretreatment of raw ramie fibers using an acidic deep eutectic solvent to produce cellulose nanofibrils in high purity," *Cellulose* 28(1), 175-188. DOI: 10.1007/s10570-020-03538-3

Zhou, Y. G., Wang, L. J., Dong, L., Yan, P. Y., Li, Y., Shi, J., Chen, X. D., and Mao, Z. H. (2009). "Effect of sucrose on dynamic mechanical characteristics of maize and potato starch films," *Carbohydrate Polymers* 76(2), 239-243. DOI: 10.1016/j.carbpol.2008.10.016

Article submitted: March 28, 2022; Peer review completed: May 22, 2022; Revisions accepted: May 26, 2022; Published: May 31, 2022.
DOI: 10.15376/biores.17.3.4347-4359